THE JOURNAL OF BIOLOGICAL CHEMISTRY
Vol. 272, No. 4, Issue of January 24, pp. 2291–2299, 1997
Printed in U.S.A.

Determination of the Solution Structures of Conantokin-G and Conantokin-T by CD and NMR Spectroscopy*

(Received for publication, June 18, 1996, and in revised form, September 5, 1996)

Niels Skjærbæk, Katherine J. Nielsen, Richard J. Lewis, Paul Alewood‡, and David J. Craik§

From The Centre for Drug Design and Development, The University of Queensland, Brisbane, Qld 4072, Australia

Conantokin-G and conantokin-T are two paralytic polypeptide toxins originally isolated from the venom of the fish-hunting cone snails of the genus *Conus*. Conantokin-G and conantokin-T are the only naturally occurring peptidic compounds which possess *N*-methyl-D-aspartate receptor antagonist activity, produced by a selective non-competitive antagonism of polyamine responses. They are also structurally unusual in that they contain a disproportionately large number of acid labile post-translational γ-carboxyglutamic acid (Gla) residues. Although no precise structural information has previously been published for these peptides, early spectroscopic measurements have indicated that both conantokin-G and conantokin-T form α-helical structures, although there is some debate whether the presence of calcium ions is required for these peptides to adopt this fold. We now report a detailed structural study of synthetic conantokin-G and conantokin-T in a range of solution conditions using CD and ^{1}H NMR spectroscopy. The three-dimensional structures of conantokin-T and conantokin-G were calculated from ^{1}H NMR-derived distance and dihedral restraints. Both conantokins were found to contain a mixture of α- and 3_{10} helix, that give rise to curved and straight helical conformers. Conantokin-G requires the presence of divalent cations (Zn^{2+}, Ca^{2+}, Cu^{2+}, or Mg^{2+}) to form a stable α-helix, while conantokin-T adopts a stable α-helical structure in aqueous conditions, in the presence or absence of divalent cations (Zn^{2+}, Ca^{2+}, Cu^{2+}, or Mg^{2+}).

Conantokin-G (con-G)[1] and conantokin-T (con-T) are highly conserved polypeptides originally isolated from the venoms of piscivorous cone snails *Conus geographus* (1) and *Conus tulipa* (2), respectively. These polypeptides are just two components in the very complex venom that these snails have developed for rapidly immobilizing their fast moving prey (3). Evidence indicates that both con-G and con-T possess *N*-methyl-D-aspartate receptor (NMDA receptor) antagonist activity, produced by a selective non-competitive antagonism of polyamine enhancement of NMDA receptor agonist activity (4–7). To date, these are the only naturally occurring peptides known to have this property. Con-G and con-T are also structurally unusual, in that they lack the disulfide motifs commonly found in conotoxin peptides and instead contain a high proportion of the base-stable but acid-labile γ-carboxyglutamic acid (Gla) residue (8, 9). Gla residues were originally identified in the vitamin K-dependent blood-clotting factors including prothrombin. Subsequently they were found in other vertebrate proteins such as osteocalcin (calcium-binding protein) (10, 11) and have been implicated in Ca^{2+} binding (12, 13). The discovery of Gla residues in several *Conus* peptides has established that this post-translational modification has a much wider phylogenetic distribution than previously thought (14).

Although no precise structural information has yet been published for these peptides using either high field NMR or x-ray techniques, previous CD spectroscopic measurements have indicated that con-G and con-T are folded in a stable α-helical conformation (7, 9). However, there is some dispute over whether these structures are stabilized by Ca^{2+} (4, 7) and furthermore, whether Ca^{2+} is essential to the biological function of the conantokin peptides (7). To investigate this intriguing problem we have synthesized con-G and con-T using Boc chemistry and investigated their solution structures in detail by CD and ^{1}H NMR spectroscopy. The effects of the solution environment including pH, monovalent cation (K^+), divalent cations (Zn^{2+}, Ca^{2+}, Cu^{2+}, and Mg^{2+}), EDTA, and TFE on the structures of con-G and con-T were monitored by CD spectroscopy. Both peptides were also examined under several conditions by ^{1}H NMR spectroscopy and their three-dimensional structures were calculated based on the NMR-derived restraints.

EXPERIMENTAL PROCEDURES

Chemicals and Reagents

All coded Boc-*L*-amino acids and reagents used during chain assembly were peptide synthesis grade supplied by Auspep Ptd. Ltd. (Parkville, Victoria). Acetonitrile (HPLC grade) was purchased from Laboratory Supply Pty. Ltd. (Coorparoo, Queensland). Deionized water was used throughout and prepared by a Milli-Q water purification system (Millipore, Waters). Screw-cap glass peptide synthesis reaction vessels (10 ml) with a sintered glass filter were obtained from Embel Scientific Glassware (Queensland). An all-Kel-F apparatus (Peptide Institute, Osaka, Japan) was used for HF cleavage. Argon, helium, and nitrogen were all ultrapure grade (CIG, Australia).

Peptide Synthesis

The sequences of the two conantokins are: conantokin-G, Gly-Glu-**Gla**-**Gla**-Leu-Gln-**Gla**-Asn-Gln-**Gla**-Leu-Ile-Arg-**Gla**-Lys-Ser-Asn-NH_2; and conantokin-T, Gly-Glu-**Gla**-**Gla**-Tyr-Gln-Lys-Met-Leu-**Gla**-Asn-Leu-Arg-**Gla**-Ala-Glu-Val-Lys-Lys-Asn-Ala-NH_2. The linear conanto-

* This work was supported in part by a research grant from the Alfred Benzon Foundation, Østbanegade, Copenhagen, Denmark (to N. S.), a Generic Industry Research and Development grant from the Australian Department of Industry, Science and Technology, and AMRAD Corporation Ltd. The costs of publication of this article were defrayed in part by the payment of page charges. This article must therefore be hereby marked "*advertisement*" in accordance with 18 U.S.C. Section 1734 solely to indicate this fact.

The atomic coordinates and structure factors (codes 1ONU and 1ONT) have been deposited in the Protein Data Bank, Brookhaven National Laboratory, Upton, NY.

‡ To whom correspondence should be addressed: Centre for Drug Design and Development, The University of Queensland, Brisbane, Qld 4072, Australia. Tel.: 61-7-3365-1271; Fax: 61-7-3365-1990.

§ Supported by an Australian Research Council Professorial Fellowship.

[1] The abbreviations used are: con-G, conantokin-G; con-T, conantokin-T; NMR, nuclear magnetic resonance; MS, mass spectrometry; DQF-COSY, double quantum filtered correlated spectroscopy; TOCSY, total correlated spectroscopy; NOESY, nuclear Overhauser enhancement spectroscopy; Boc, *tert*-butoxycarbonyl; HF, hydrogen fluoride; Gla, γ-carboxyglutamic acid; TFE, 2,2,2-trifluoroethanol; NMDA, *N*-methyl-D-aspartate; RMSD, root mean square deviation; deg, degree.

kins were assembled manually using solid phase methodology with Boc chemistry (15). Both peptides were assembled on *p*-methylbenzhydrylamine-resin·HCl on a 0.2 mmol scale. The following side chain protected amino acids were employed: Asn(xanthyl), Lys(2-chlorobenzyloxycarbonyl), Glu(γ-cyclohexyl), Arg(*p*-toluenesulfonyl), Ser(benzyl), Gln(xanthyl), and Gla(γ-cyclohexyl)$_2$. A 4-fold excess of Boc amino acids was used based on the original substitution of *p*-methylbenzhydrylamine-resin·HCl. Boc-*L*-Gla(γ-cyclohexyl)$_2$-OH·DCHA was coupled with a 1.25 mol excess. Boc-Gla(γ-cyclohexyl)$_2$ was synthesized as described previously (8). All amino acids were activated using 2-(1*H*-benzotriazole-1-yl)-1,1,3,3-tetramethyluronium hexafluorophosphate (0.5 M in dimethylformamide) and *N*,*N*-diisopropylethylamine and coupled for 10 min, except for Boc-Gla(γ-cyclohexyl)$_2$ which was coupled for 60 min. Boc protecting groups were removed using 100% trifluoroacetic acid and the peptides were cleaved from the resin using HF.

Con-G—The peptide resin (415 mg, 94.3 mmol) was treated with HF (9 ml) in the presence of *p*-cresol (1 ml) at −5 °C for 2 h. Crude peptide was precipitated with cold ether, washed with cold ether, then extracted into 20% acetic acid and lyophilized to yield 201 mg (86%) of crude con-G. The crude peptide was purified on a conventional reverse-phase Vydac C_{18} silica preparative column using a linear gradient (0–80% B) over 80 min at a flow of 8 ml/min. Solvent A was 0.1% aqueous trifluoroacetic acid, solvent B was 90% acetonitrile/water containing 0.09% trifluoroacetic acid. Sample absorbance was recorded at 230 nm. Highly pure fractions were collected and lyophilized and pure con-G was further lyophilized 3 times from deionized water. ES-MS: $[M + H]^+$ 2264.6 (calculated 2265.2). Amino acid analysis after hydrolysis in 6 M HCl at 105 °C for 24 h: Asx 2.43 (2), Glx 8.28 (8), Ser 0.90 (1), Gly 0.91 (1), Arg 1.00 (1), Ile 0.73 (1), Leu 1.83 (2), Lys 0.93 (1).

Con-T—This peptide was prepared in a similar fashion to con-G to yield 126 mg (51%). ES-MS: $[M + H]^+$ 2684.0 (calculated 2684.9). Amino acid analysis after hydrolysis in 6 M HCl at 105 °C for 24 h: Ala 2.01 (2), Asx 2.21 (2), Glx 7.20 (7), Gly 0.98 (1), Val 1.05 (1), Met 0.93 (1), Tyr 1.07 (1), Arg 1.03 (1), Leu 1.90 (2), Lys 3.10 (3).

Mass Spectrometry

Mass spectra were acquired on a PE-SCIEX API III triple quadrupole mass spectrometer equipped with an ionspray atmospheric pressure ionization source. Mass spectra were typically acquired in 5–15 min on an Apple Macintosh IIfx computer and processed using the software package MacSpec (Sciex, Toronto, Canada). Interpretation of the spectra was aided by MacBiospec (Sciex, Toronto, Canada).

Peptide Authentication

Venom was isolated from the dissected venom ducts of individual *C. geographus* and *C. tulipa* collected on the Great Barrier Reef, Australia (16). Soluble venom components were extracted with 30% acetonitrile/water acidified with 0.1% trifluoroacetic acid, freeze-dried, and stored at −20 °C. Venom was redissolved in 5% acetonitrile/water acidified with 0.1% trifluoroacetic acid at ≈1 mg/ml prior to HPLC purification. Comparative HPLC analyses were performed on the native peptides, the synthetic peptides, and a mixture of native and synthetic peptides (1:1). HPLC analyses were performed on an analytical HPLC system (ABI 140B dual syringe pump gradient HPLC system) using a Vydac C_{18} 5-μm column (2.1 × 250 mm). Chromatograms were achieved using a linear gradient of 0–80% B over 160 min at a flow rate of 1 ml/min. Solvent A was 0.1% aqueous trifluoroacetic acid, solvent B was 90% acetonitrile/water acidified with 0.09% trifluoroacetic acid. Synthetic samples of con-G and con-T both co-eluted with the native samples (data not shown) which confirmed that the synthetic and native materials were identical.

Cation Removal

Preparative HPLC was performed immediately on a calcium loaded con-G sample ($CaCl_2$, 6.5 mM) following CD analysis. CD analysis of the repurified peptide showed no helix formation to be present. This is indicated by the lack of minima at 208 and 222 nm (data not shown). Thus HPLC chromatography under acidic conditions is sufficient to remove Ca^{2+} bound to con-G.

CD Studies

CD spectra were obtained using a Jasco spectrometer (J-710) with a 0.1-cm path length cuvette at 20 °C. Both peptides were dissolved in a 10 mM phosphate buffer (pH 7.4) at a 75 μM concentration, for all experiments. The secondary structure was estimated by analysis of the spectrum between 190 and 250 nm. Mean residue ellipticity $[\theta]_{MR}$ is expressed in degrees-square centimeter per decamole ((deg·cm^2)/dmol). Experimental estimates of helical contents were determined from the $[\theta]_{222}$ measurements. An estimate of helical content was determined using an equation developed by Chakrabartty *et al.* (17) (−40,000 (1–2.5/*n*); *n* = number of residues), where −40,000 and 0 (deg·cm^2)/dmol are the values for 100% and 0% α-helix, respectively. This equation is used only as a qualitative estimate of peptide helicity.

NMR Spectroscopy

All NMR spectra were recorded on a Bruker ARX 500 spectrometer equipped with a *z*-gradient unit. Peptide concentrations were 2 mM. Spectra of con-G were obtained in 95% H_2O, 5% D_2O with no $CaCl_2$ (pH 5.5), 1:1 (pH 5.5) and 5:1 (pH 3.5 and 5.5) ratios of $CaCl_2$ to peptide, and in 33% TFE. Spectra of con-T were obtained in 95% H_2O, 5% D_2O with no $CaCl_2$ (pH 5.5) and a 5:1 (pH 5.5) ratio of $CaCl_2$ to peptide, and in 33% TFE. ^{1}H NMR spectra recorded were DQF-COSY (18), NOESY (19, 20) with mixing times of 100–300 ms and TOCSY (21) with a mixing time of 65 ms. All spectra were recorded at 280 K, except for some additional spectra at 298 K. Spectra were run over 6024 Hz with 4 K data points, 400–600 free induction decays, 16–64 scans, and a recycle delay of 1 s (1.5 s for DQF-COSY). In NOESY and TOCSY spectra, the solvent was suppressed using the WATERGATE sequence (22). Spectra were processed using UXNMR. Free induction decays were multiplied by a polynomial function and apodized using a 60 or 90 ° shifted sinebell function in both dimensions prior to Fourier transformation. Baseline correction using a fifth polynomial was applied and chemical shift values were referenced externally to 4,4-dimethyl-4-silapentane-1-sulfonate at 0.00 ppm. $^3J_{NH\text{-}H\alpha}$ coupling constants were measured from high resolution one-dimensional spectra (32 K) and compared to those obtained from the DQF-COSY spectra which were strip transformed to 8K × 1K and extracted using the Lorentzian line-fitting routine in the program Aurelia (Bruker GMBH).

Distance Restraints and Structure Calculations

Peak volumes in NOESY spectra were classified as strong, medium, weak, or very weak corresponding to upper bounds on interproton distances of 2.7, 3.5, 5.0, or 6.0 Å, respectively. Lower distance bounds were set to 1.8 Å. Appropriate pseudoatom corrections (23) were made and distances of 1.5 Å and 2.0 Å were added to the upper limits of restraints involving methyl and phenyl protons, respectively. $^3J_{NH\text{-}H\alpha}$ coupling constants were used to determine ϕ dihedral angle restraints (24).

Structures were calculated (coordinates have been deposited with the Brookhaven Protein Databank) using the simulated annealing protocol in X-PLOR (25, 26) version 3.1 using the geometric forcefield, parallhdg.pro. Starting structures were generated using random (ϕ, ψ) dihedral angles and energy minimized (500 steps) to produce structures with correct local geometry. The structures were subjected to a total of 30 ps of high temperature molecular dynamics before cooling and energy minimization (1000 steps). Structure refinements were performed using energy minimization (2000 steps) under the influence of the CHARMM forcefield (27).

Data Analysis

Structures were compared using pairwise and average RMSDs for the Cα, C, and N atoms (X-PLOR version 3.1) and by calculating angular order parameters for the backbone dihedral angles (28, 29). Structure visualization was performed using INSIGHT II (Biosym Technology Inc.).

RESULTS

Circular Dichroism Spectroscopy—CD spectra were used as a qualitative gauge of peptide secondary structure. The CD spectra of con-G and con-T both exhibit minima at 208 and 222 nm at high concentrations of $CaCl_2$ (9.2 and 4.5 mM, respectively), which is the characteristic signature for α-helix. Increasing the $CaCl_2$ concentration further did not enhance the α-helix content in either peptide, nor did the addition of 50% TFE to the $CaCl_2$ (9.2 mM) solution of con-G (Fig. 1*A*). For con-G, there is clearly a $CaCl_2$ concentration dependence. In the absence of $CaCl_2$ almost no helical structure was observed (7%) but on increasing the $CaCl_2$ concentration, the percentage of helical structure rose steadily to a maximum of 45% (Fig. 1*A*). In contrast, when this experiment was performed with con-T, no $CaCl_2$ concentration dependence was observed. Instead, con-T showed a high degree of helical content (50%) in

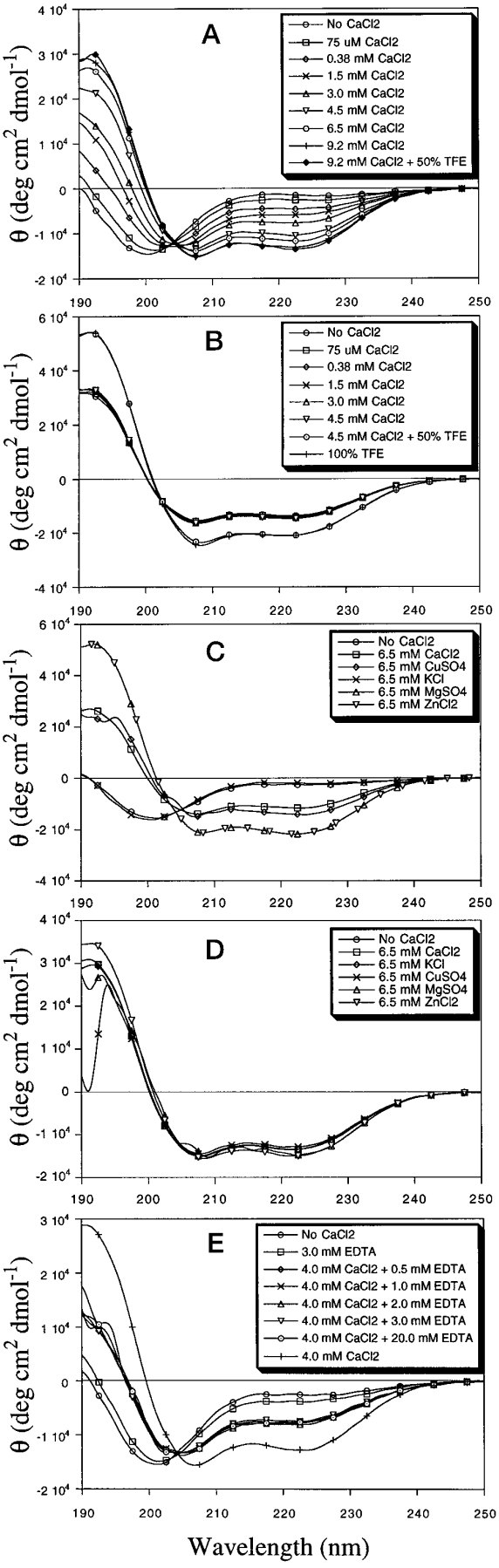

FIG. 1. **CD spectra of con-G and con-T under different conditions.** *A,* CD spectra of con-G obtained at different $CaCl_2$ concentrations. *B,* CD spectra of con-T obtained at different $CaCl_2$ concentrations. *C,* CD spectra of con-G obtained with different metal ions. *D,* CD spectra of con-T obtained with different metal ions. *E,* CD spectra of con-G with fixed $CaCl_2$ concentration and different EDTA concentrations.

buffer solution alone (Fig. 1*B*). Although the addition of $CaCl_2$ did not affect the percentage of α-helix present in con-T, the addition of 50% TFE to a 4.5 mM $CaCl_2$ solution increased the α-helical content to 63%. The same result was obtained in 100% TFE (Fig. 1*B*).

As the conantokin peptides apparently bind to, or affect allosterically, the putative combined polyamine/Mg^{2+} binding site on the NMDA receptor (30, 31), it was of interest to determine the effects of Mg^{2+} on the structure of con-G and con-T and to explore the possibility that other positively charged ions could stabilize the structures in the same manner as $CaCl_2$. The CD spectra showing the effects of cation concentration on con-G are given in Fig. 1*C*. As anticipated, monovalent potassium ion did not stabilize the structure of con-G. On the other hand, Cu^{2+} stabilizes the peptide as efficiently as Ca^{2+}. Most striking were the effects of Mg^{2+} and Zn^{2+}, which provided greater stabilization to the con-G structure than Ca^{2+}, with estimated α-helix contents of 68 and 69%, respectively. As seen in Fig. 1*D*, different cations did not significantly affect the helical content of con-T, which was estimated to be 50%.

CD spectra showing the effects of the addition of EDTA to a fixed concentration of peptide (con-G) and $CaCl_2$ are given in Fig. 1*E*. In this experiment, the degree of α-helix present for con-G in $CaCl_2$ is substantially decreased by the presence of EDTA. This indicates that EDTA chelates some of the $CaCl_2$. However, the minimum α-helix content is greater than that calculated for con-G in buffer alone, even when a large excess of EDTA (20 mM) is added to the $CaCl_2$ solution. Furthermore, it was shown that addition of 3.0 mM EDTA to a con-G solution with no $CaCl_2$ present had no effect on the peptide structure.

The CD results show that the structure of con-T is predominantly helical in aqueous buffer and more so in TFE. Cations such as Ca^{2+}, Cu^{2+}, K^+, Mg^{2+}, and Zn^{2+} have no significant effect on the helix content of this peptide (Fig. 1*D*). In contrast, the structure of con-G, which is not highly helical in buffer, is greatly affected by the presence of Ca^{2+}, presumably with the Gla residues being involved in the Ca^{2+}-binding interaction. For con-G, the degree of helicity correlated to the amount of Ca^{2+} present. In the presence of excess EDTA, there is apparently substantial Ca^{2+} which remains chelated to the peptide, either inaccessible to, or in equilibrium with, EDTA. The CD studies show that con-G is selective for divalent cations, with monovalent cations having little influence on the structure of this peptide. No cation selectivity was observed for con-T. This study provides evidence that Mg^{2+} and Zn^{2+} induce greater helical content than Ca^{2+} and Cu^{2+} in con-G.

NMR Spectroscopy

Chemical Shift Assignment—Due to the large number of residues with similar spin-types the two-dimensional spectra of con-G and, to a lesser extent con-T, are severely overlapped under the conditions used. Despite this, assignment was possible by a careful analysis of NOESY, TOCSY, and DQF-COSY spectra (23). An example of the NOESY spectrum of con-G in H_2O showing the sequential assignment is given in Fig. 2. The complete chemical shift assignments of con-G and con-T are supplied as supplementary material.

Secondary Hα Shifts—The deviations of Hα chemical shifts from their random coil values provide information on peptide backbone structure (23, 32). For con-G in H_2O, there are some large negative secondary Hα shifts indicative of α-helix from

Asn^8 to the C terminus (Fig. 3). The magnitude of the secondary shift is greatest in region 9–13. The addition of TFE did not alter the pattern of secondary shift, but greatly enhanced the magnitude of secondary shift for each residue, indicating that the α-helix is stabilized over the entire peptide. Similarly, the addition of $CaCl_2$ to con-G accentuated the negative secondary shifts. At pH 3.5, the secondary shifts of residues 5–6 and 8–9 are enlarged, while at pH 5.5, α-helix is further stabilized over the whole peptide. This is consistent with the Ca^{2+}-induced secondary structure stabilization. Furthermore, since the helix content increased at a higher pH, this suggests that the Ca^{2+} binds to the negatively charged Gla side chains.

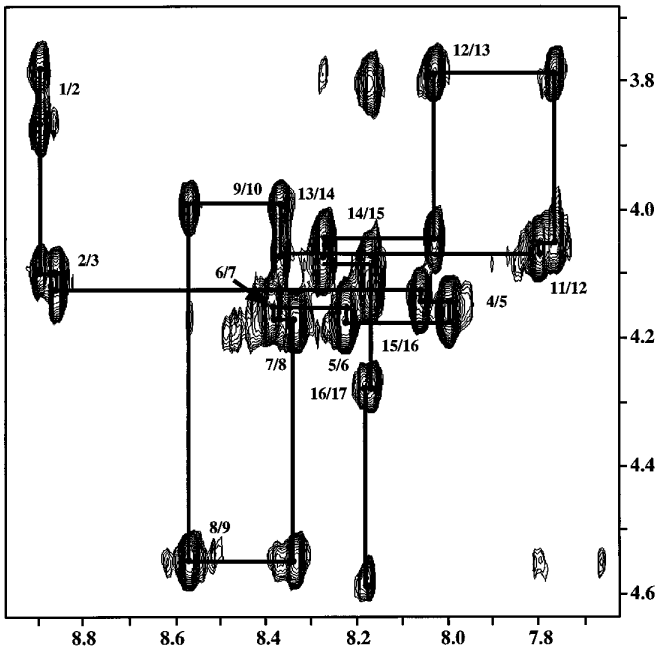

FIG. 2. **NOESY spectrum of con-G in the NH-Hα region.** The NH-Hα region of the NOESY spectrum (mixture = 300 ms) of con-G in H_2O (T = 280 K; pH 5.5) showing the sequential connectivities.

The large negative secondary Hα shifts of con-T (Fig. 4) indicate that this peptide is extremely helical, even in H_2O (residues 3–21) and more so in TFE (residues 2–21). The effects of Ca^{2+} on the Hα shifts were minimal, supporting the CD data which clearly indicated that there was no overall structural stabilization in this case. However, an exception to this is the secondary Hα shift of Gla^{10}, which is shifted to a positive value, in the presence of Ca^{2+} at pH 5.5. It is noteworthy that this is also observed for con-G, under the same conditions. Although this implies helix disruption, it may instead be due to an underestimate of the random coil shift of Gla (this is not available in the literature and the value for Glu was used in its place).

NOEs—A summary of the observed sequential and medium-range NOEs for con-G is given in Fig. 5. No long range NOEs were detected under any of the conditions used. Although many medium-range NOEs (Hα-Hβ_{i+3}, Hα-HN$_{i+2}$, and HαHβ_{i+3}) were present, consistent with α-helical secondary structure, the peak overlap meant that it was not possible to detect many NOEs that may be expected based on the extent of α-helix deduced from the chemical shift data. This is most evident in the data collected at pH 5.5 in the presence of Ca^{2+}. In this case, the combined effects of large line widths and peak overlap were deleterious to spectral quality, resulting in few observable connectivities in the NH-Hα region. Increasing the temperature to 298 K sharpened the line widths, however, the accompanying decrease in correlation time resulted in low NOE intensities. Despite this, from decreases in the Hα-NH$_{i+1}$/NH-NH$_{i+1}$ ratios, and from the observation of key medium-range NOEs, it is clear that the α-helical content, present over the region encompassed by residues 5–17 in the absence of $CaCl_2$, increased in the presence of $CaCl_2$ to incorporate the entire peptide. In particular, the strengths of the non-overlapped Hα-Hβ_{i+3} NOEs, *i.e.* from Leu^5-Asn^8 and Gla^{10}-Gla^{14} increase significantly in the presence of $CaCl_2$ at pH 5.5. At pH 3.5 and in the presence of $CaCl_2$ there is less difference in NOE strengths compared with con-G at pH 5.5, providing further

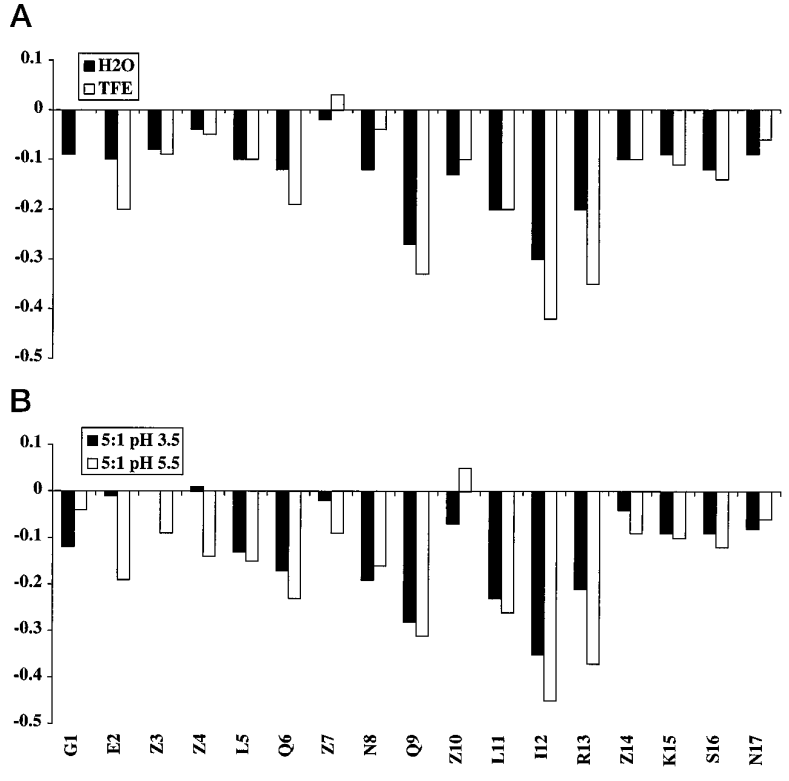

FIG. 3. **Secondary Hα shifts for con-G under different conditions.** Secondary Hα shifts in ppm (*y* axis), calculated using the random coil shifts of Merutka *et al.* (37) for (*A*) con-G in H_2O and TFE and (*B*) con-G with 5:1 $CaCl_2$ at pH 3.5 and 5.5. The Glu random coil Hα chemical shift was substituted for that of Gla which is not known.

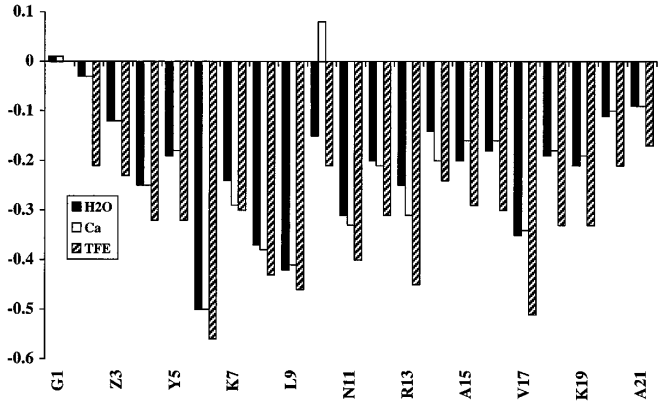

FIG. 4. **Secondary Hα shifts for con-T under different conditions.** Secondary Hα shifts in ppm (*y* axis), calculated using the random coil shifts of Merutka *et al.* (37) for con-T in H_2O, $CaCl_2$, and TFE. The Glu random coil Hα chemical shift was substituted for that of Gla which is not known.

support that the Gla side chains need to be charged for optimal helix stability and Ca^{2+} chelation.

The two-dimensional spectra of con-T were more dispersed in the NH region than those of con-G. Consequently, it was possible to observe many more NOEs (Fig. 6). In H_2O, the large number of characteristic Hα-NH_{i+3}, Hα-NH_{i+4}, Hα-NH_{i+2}, and Hα-$H\beta_{i+3}$ NOEs, medium-strong NH-NH_{i+1} and medium Hα-NH_{i+1} NOEs show that con-T adopts α-helix from residues 2 to 21. The helix enhancement in the presence of TFE is suggested by the slightly weaker Hα-NH_{i+1} relative to NH-NH_{i+1} NOEs. However, the addition of TFE caused a reduction in NH shift dispersion so that many connectivities are not detectable.

$^3J_{NH\text{-}H\alpha}$ Coupling Constants and Slow Exchange Data—The $^3J_{NH\text{-}H\alpha}$ coupling constant and NH slow exchange data augment the NOE information. Over the range of solution conditions, it was possible to obtain $^3J_{NH\text{-}H\alpha}$ data for all residues of both peptides. Consistent with well defined α-helix, all measurable $^3J_{NH\text{-}H\alpha}$ coupling constants are low (<6 Hz) in con-T apart from that of Asn^{20}. Similarly, for con-G, all $^3J_{NH\text{-}H\alpha}$ coupling constants are low except for Ser^{16} and Asn^{17} which are only slightly larger (<7 Hz), reflecting some degree of conformational averaging at the C terminus. The extent and stability of helix is further demonstrated by the large proportion (13/20) of NH protons of con-T which were observed to be slowly exchanging in aqueous solution, despite the relatively high pH. Similarly, several (7/16) of the NH protons of con-G in $CaCl_2$ also exchanged slowly with solvent.

Three-dimensional Structure of Conantokin Peptides

The secondary structure analysis indicates that con-G adopts transient α-helix in aqueous solution which is stabilized by the presence of Ca^{2+}, although the CD analysis indicates that other divalent cations will suffice or even improve helix stabilization. In contrast, con-T forms a stable α-helix in aqueous solution in the absence or presence of divalent counterions. The conditions needed for these peptides to adopt what is presumably their inherently preferred conformational state are different, however, the qualitative study described above suggests that their three-dimensional structures are similar. This may also be inferred from high sequence identity in the N-terminal region and from the similarity of their biological activity. A quantitative comparison of con-G and con-T based on the computation of their three-dimensional structures is described below.

Three-dimensional Structure of Conantokin-G—A total of 161 distance restraints (58 intra residual, 60 sequential, and 43 medium range) and 14 dihedral restraints were used in the calculation of 30 structures. Of these structures 18 had no NOE

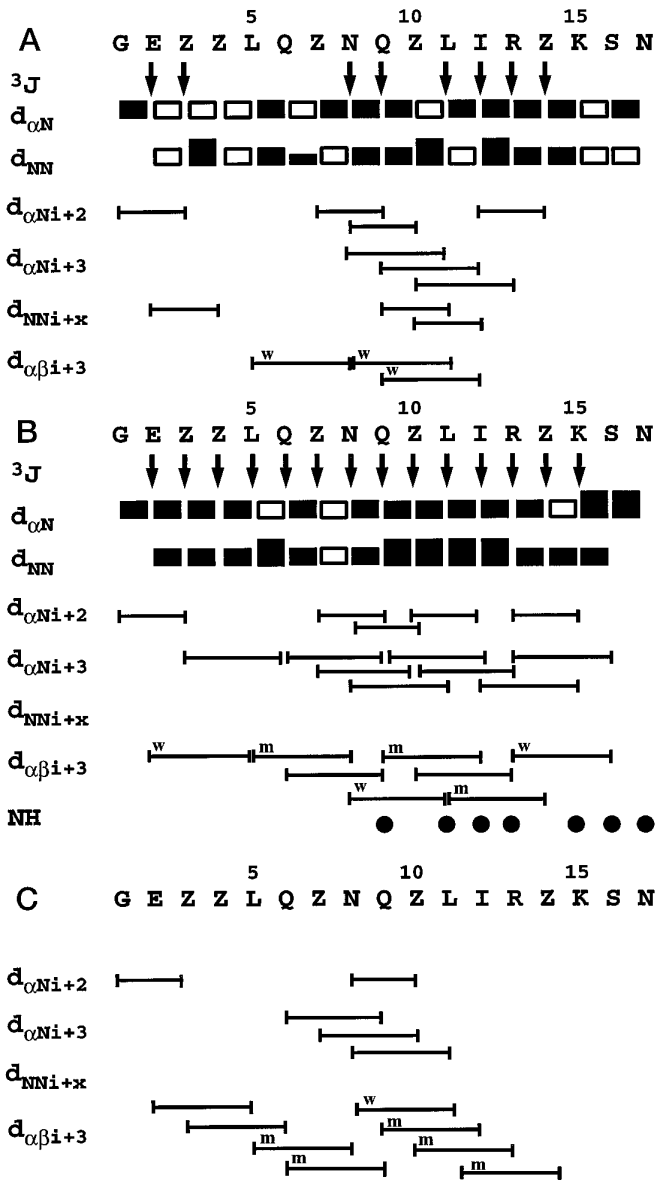

FIG. 5. **Sequential NOEs for con-G under different conditions.** A summary of sequential NOEs for con-G in (*A*) H_2O, pH 5.5; (*B*) 5:1 $CaCl_2$, pH 3.5; and (*C*) 5:1 $CaCl_2$, pH 5.5. Thickness of the *bars* represent the strength of the NOE connectivities and *unshaded bars* represent peak overlap. Also shown are medium range NOE connectivities, $^3J_{NH\text{-}H\alpha}$ coupling constants and slow exchange NH protons (*filled circles*). $^3J_{NH\text{-}H\alpha}$ coupling constants were unobtainable in the 5:1 $CaCl_2$: peptide solution (pH 5.5), due to large line widths. Slow exchange data were obtained only for *B*, as the data from which 30 structure restraints were obtained.

violations greater than 0.2 Å and no dihedral violations greater than 3° and were chosen to represent the structure of con-G. The structures satisfy the experimental and empirical criteria as the average deviations from ideal covalent geometry and experimental restraints are low and the potential-energy and restraint energy contributions are favorable (Table I). While the backbone pairwise RMSD is high over the whole molecule, the RMSDs over each half are much lower (Table I), suggesting that the helix has some flexibility. This can also been seen from the backbone angular order parameters and RMSD values for individual residues shown in Fig. 7*A*. The angular order parameters are high over residues 2–15, indicating consistency in local geometry among the structures. As is usual with linear peptides, there are elevated RMSDs at the termini consistent with some helix fraying. The RMSD values are lowest in two

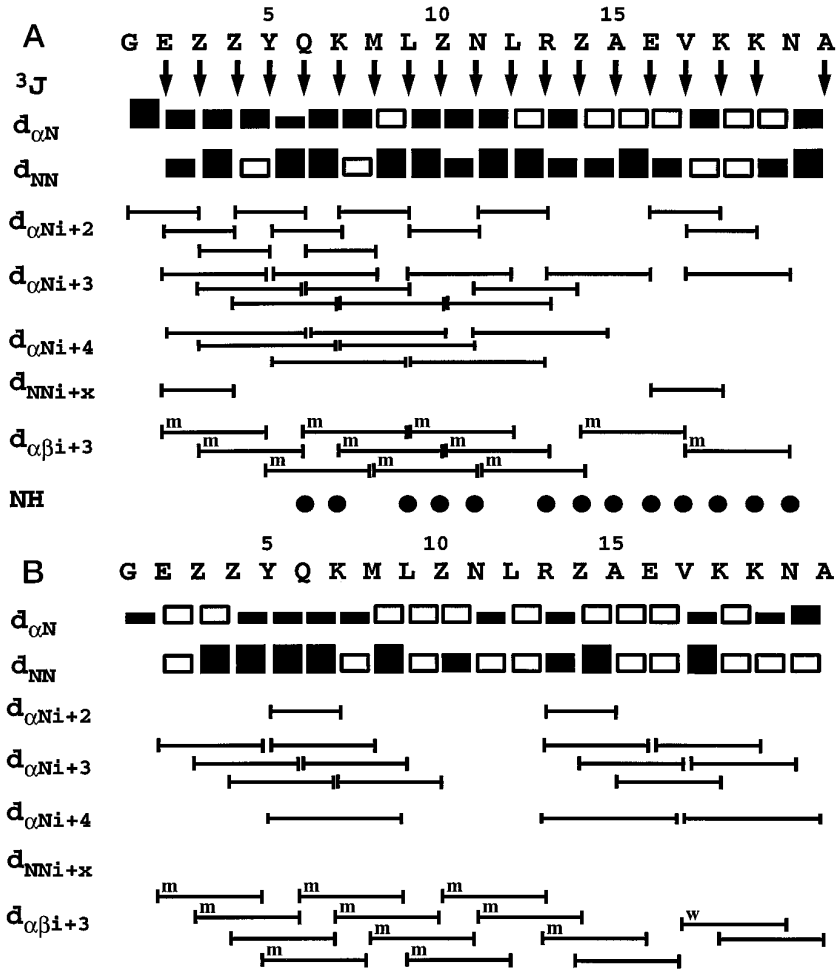

FIG. 6. **Sequential NOEs for con-T under different conditions.** A summary of sequential NOEs for con-T in (*A*) H_2O, pH 5.5; and (*B*) 30% TFE. *Thickness* of the *bars* represent the strength of the NOE connectivities and *unshaded bars* represent peak overlap. Also shown are medium range NOE connectivities, $^3J_{NH\text{-}H\alpha}$ coupling constants and slow exchange NH protons (*filled circles*). $^3J_{NH\text{-}H\alpha}$ coupling constants and slow exchange NH protons were not obtained for *B* due to large line widths and weak signals in TOCSY experiment.

TABLE I
Geometric and energetic statistics for the conantokin structures

	Conantokin-G	Conantokin-T
Average RMSD to mean structure	1.68 Å	1.86 Å
Pairwise RMSD for Cα, N, C atoms		
All residues	2.46 Å	1.71 Å
N terminus	1.22 Å (residues 2–9)	0.67 Å (residues 2–10)
C terminus	0.85 Å (residues 10–17)	0.86 Å (residues 13–20)
RMSDs from distance restraints	0.010 ± 0.004 Å	0.016 ± 0.006 Å
RMSDs from dihedral restraints	0.11 ± 0.12°	0.17 ± 0.13°
RMSDs from idealized geometry		
Bonds (Å)	0.010 ± 0.001	0.009 ± 0.001
Angles (°)	1.88 ± 0.08	2.01 ± 0.10
Impropers (°)	0.14 ± 0.03	0.11 ± 0.03
Energies (kcal mol^{-1})		
E_{NOE}	0.53 ± 0.58	2.08 ± 1.60
E_{cdih}	0.022 ± 0.038	0.056 ± 0.074
$E_{L\text{-}J}$	−94.1 ± 11.4	−121.4 ± 13.9
$E_{bond} + E_{angle} + E_{improper}$	29.6 ± 2.9	41.6 ± 4.5

sections of the peptide (residues 5–6 and 9–14), but elevated at residues 7–8.

It is evident from a series of backbone superimpositions (Fig. 8) over particular regions, that the helix of con-G is highly defined over segments of up to 8 residues. Superimpositions of the middle segment of the peptide highlights the good definition but leaves an exaggerated impression of frayed termini. However, superimpositions in regions around the N or C terminus show clearly that helix is relatively well defined at both termini (Fig. 8). This is upheld by analysis of the backbone ϕ-ψ coordinates which shows that all residues lie in the α-region of the Ramachandran plot. While the individual three-dimensional structures of con-G each consist of unbroken helix, few of the helices are linear, with most having some form of kink or curvature. This implies that either the NMR data are not sufficient to define the relative orientations of sections of the helix, or that the long helix has genuine flexibility. The high degree of curvature observed in most of our structures is not surprising, as this is commonly observed for amphipathic helices in solution (33, 34). Analysis of the backbone H-bonds shows that all structures contain a mixture of i,i+3, and i,i+4 interactions, consistent with 3_{10} and α-helix, respectively, where the 3_{10} helix component consists of approximately 38% of the total backbone H-bonds.

Three-dimensional Structure of Conantokin-T—A set of 17/30 structures was chosen to represent con-T, based on the

criterion stated above, using 255 distance restraints (91 intra-residual, 89 sequential, and 75 medium range) and 19 dihedral restraints. The deviations from ideal geometry and from experimental restraints are given in Table I, together with backbone pairwise RMSD values. These are lower than for con-G, reflecting the greater number of distance restraints per residue used in the calculations. Again, the pairwise RMSD values are substantially lower when the N terminus, middle segment, and C terminus are treated separately. These regions are shown superimposed in Fig. 9. The backbone angular order parameters (Fig. 7*B*) are consistently high for residues 2–21, which all lie in the α-region of the Ramachandran plot. The backbone RMSD values (Fig. 7*B*) are lowest for residues 4–9 and 16–18. The central region 10–14 of the peptide has elevated RMSD values, most likely due to some flexibility in this region. Similar to con-G, most of the helices are nonlinear, with the degree of curvature varying significantly. H-bond analysis again indicates that a mixture of 3_{10} and α-helix is present, with the 3_{10} helix component representing approximately 30% of the total measured backbone H-bonds.

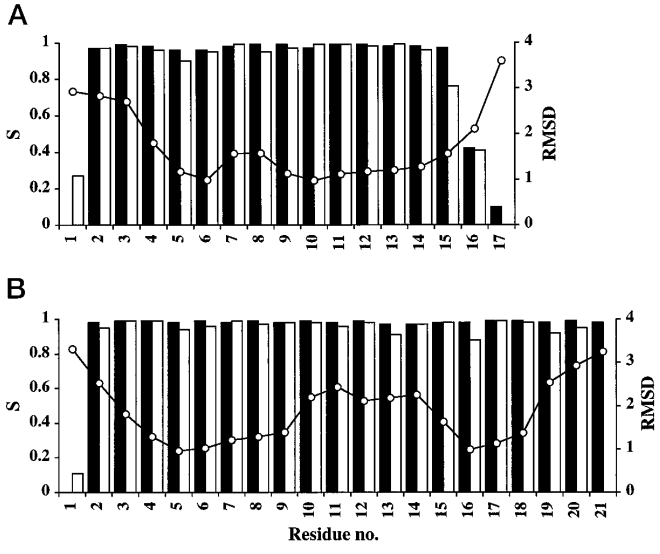

FIG. 7. **Backbone angular order parameters for con-G (*top panel*) and con-T (*lower panel*).** The backbone angular order parameters for *A*, con-G showing: S(ϕ) (*shaded*) and S(ψ) (*outline*) and backbone RMSD *versus* residue number; and *B*, for con-T showing the backbone angular order parameters S(ϕ) (*shaded*) and S(ψ) (*outline*) and backbone RMSD *versus* residue number.

DISCUSSION

Divalent Cation Concentration—The CD spectra of both con-G and con-T shown in Fig. 1, *A* and *B*, indicate that these peptides are strongly helical in the presence of Ca^{2+}. The most striking observation is that con-T is extremely helical, even in the absence of Ca^{2+}, which may be explained by the relative positions of the Gla residues (see below). The EDTA titrations showed that some of the Ca^{2+} ions are bound very tightly to con-G, even when the EDTA concentration is increased to four times the concentration of $CaCl_2$. At these relative concentrations, the peptide still exhibits residual Ca^{2+}-induced stabilization. EDTA did not reduce the helical content below that induced by 3.0 mM $CaCl_2$. This shows that Ca^{2+}, in some instances, is bound more tightly to con-G than to EDTA.

Potassium ions did not stabilize the peptides (Fig. 1, *C* and *D*), due to their different ionic properties relative to Ca^{2+}. Of the divalent cations, Mg^{2+} and Zn^{2+} provided the greatest stabilization to the structure of con-G.

Comparison of the Structures of Con-G and Con-T—The results have shown that con-G and con-T both adopt stable helices over their entire length, although the conditions required to achieve this are slightly different. The three-dimensional structures of both peptides show that although each residue is well defined locally, there are a range of global orientations that agree with the experimental restraints. A superimposition of con-G curved and linear structures with corresponding structures of con-T (Fig. 10*A*) emphasizes a striking degree of similarity. A surface representation of a typical curved structure for each of con-G and con-T in identical orientations in Fig. 10*B* shows the hydrophilic residues, at least from residues 3 to 13, are on the exterior surface and the hydrophobic residues are on the inner (more concave) surface, a phenomenon which is a characteristic feature of amphipathic helices in solution. The hydrophobic face of both peptides are alike, being composed of a mixture of polar and hydrophobic side chains. Characteristic of amphipathic helices, the hydrophilic face of con-T consists of alternating regions of positive and negative charge, however, that of con-G is unusual in that it consists almost entirely of negative charge. Presumably, the binding of divalent cations to this region of con-G stabilizes a conformational state that would otherwise be unfavorable electrostatically. In contrast, con-T does not require Ca^{2+} to adopt the same conformation, although it does not necessarily follow that Gla side chains in this peptide do not bind to divalent cations.

The three-dimensional structures of con-G and con-T are

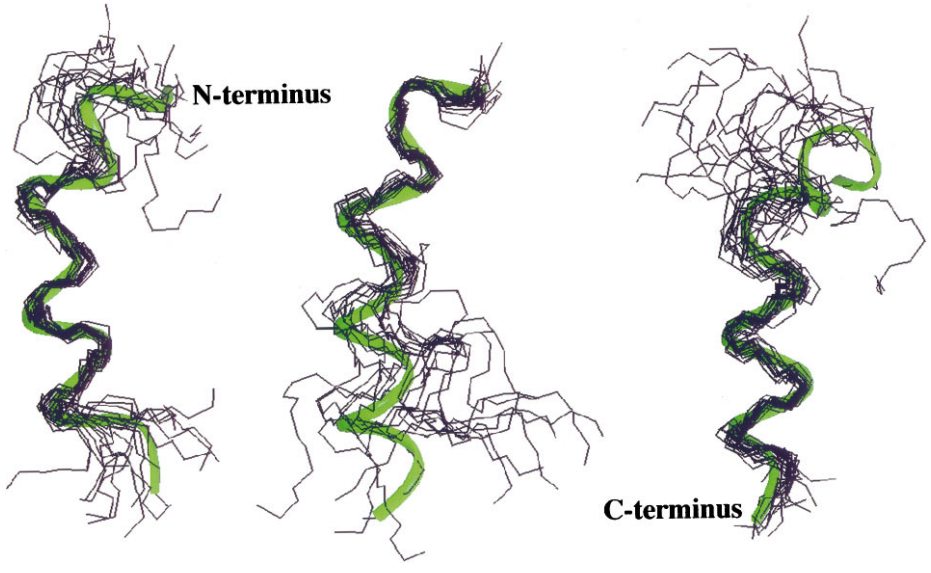

FIG. 8. **The 18 low energy structures of con-G showing superimpositions over residues 6–14 (*left*), 2–9 (*middle*), and 11–16 (*right*).** Shown in green ribbon are three different low energy structures that represent con-G.

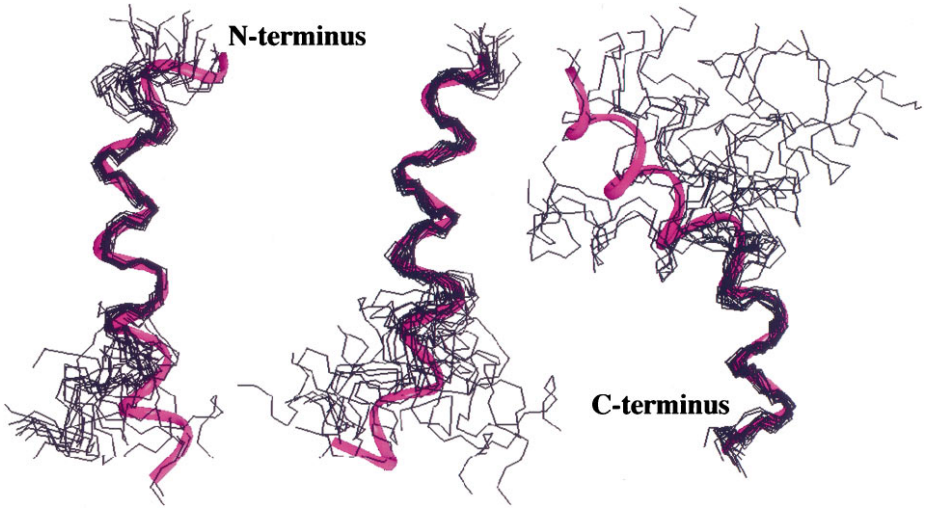

FIG. 9. **The 17 low energy structures of con-T showing superimpositions over residues 6–14 (*left*), 2–10 (*middle*), and 11–20 (*right*).** Shown in pink ribbon are three different low energy structures that represent con-T.

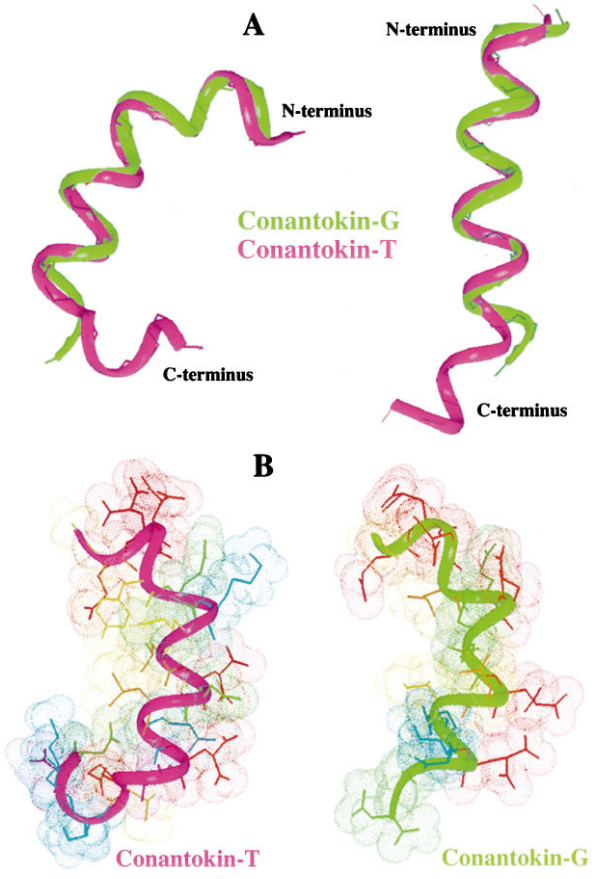

FIG. 10. *A,* backbone superimpositons of two low energy structures of con-G (green) and con-T (pink) over residues 2–14 representing curved (*left*) and linear (*right*) helices; and *B*, surface views of low energy structures of con-G (green) and con-T (pink). Color coding is as follows: positively charged residues, blue; negatively charged residues, red; polar residues, green; hydrophobic residues, yellow. Although the local geometry of the side chains are not well defined, their relative positions are similar in each of the structures.

composed of a dynamic mixture of 3_{10} and α-helix. Although theoretical studies on the relative energies of 3_{10} *versus* α-helix suggest that the latter conformation is preferred in helices of greater than 10–12 residues due to a lower degree of steric hindrance (35, 36), this is offset in con-T by a large number of putative electrostatic i,i+3 interactions which would favor 3_{10} helix formation. For example, helix stabilizing salt-bridges may be formed between Gla^4-Lys^7, Lys^7-Gla^{10}, Gla^{10}-Arg^{13}, Arg^{13}-Glu^{16}, and Glu^{16}-Lys^{19} in the 3_{10} conformation, but only between Gla^3-Lys^7 and Gla^{14}-Lys^{18} in α-helix. Furthermore, in the α-helical conformation, the Gla^{10}-Gla^{14} interaction would be disruptive. The same argument may be applied to con-G to explain why it is less helical in the absence of divalent cations. The electrostatic repulsion of the side chains of Gla^3-Gla^7, Gla^4-Gla^7, Gla^7-Gla^{10}, and Gla^{10}-Gla^{14} would hinder both 3_{10} and α-helical conformations. However, the presence of Ca^{2+} could promote the alignment of Gla residues so that the above mentioned interactions become favorable.

Comparison with Previous Reports on Conantokin Structures—This is the first published report on the three-dimensional structure of con-G and con-T, however, there have been previous CD spectroscopic studies of both peptides (4, 7). Zhou *et al.* (7) suggest that con-G adopts a highly characteristic helix with a rigid middle segment and mobile N- and C-terminal ends. They propose that the middle segment may function as a helical spacer between the two flexible terminal domains that may bind to two separate sites on the NMDA receptor (7). This suggestion may be regarded as tentative, as CD spectroscopy does not provide structural information in a sequence specific manner. The NMR data presented here provides sequence specific structural information and shows that the helix extends from the N to the C terminus. In addition, the helical region is not necessarily rigid, even in the middle segment, but may have considerable flexibility arising from α-helix to 3_{10}-helix transitions. This $\alpha \leftrightarrow 3_{10}$ interchange was also proposed by Zhou *et al.* (7) on the basis of their CD studies of con-G analogues with specific Gla → Ala, Gla → Ser, or Gla → phospho-Ser (3_{10} helix inducing) substitutions.

Role of Divalent Cations—Of significant importance is the role divalent cations play in structure-activity relationships for the conantokins. In the case of con-G, we find there is a structural dependence on divalent cation concentration, however, this is not consistent with the recent findings of Chandler *et al.* (4) and Zhou *et al.* (7). In both these earlier studies, the helix content determined by CD spectroscopy for con-G in the absence of added Ca^{2+} is approximately equivalent to that calculated here for the peptide in the presence of excess Ca^{2+}. This strongly suggests that some Ca^{2+}, or perhaps another divalent cation, was already bound to con-G prior to the addition of Ca^{2+}. Indeed, our experiments with EDTA show that Ca^{2+} bound to con-G is difficult to remove. Considering this and also the range of divalent cations which have been shown here to affect the stability of the con-G structure, the validity of recent activity experiments performed in the "nominal" absence of Ca^{2+} are open to question (6). The role of the divalent cations

seems more problematic by the finding that the structure of con-T does not appear to be affected by the addition of Ca^{2+}. However, the lack of structural stabilization does not exclude divalent cations from binding to the Gla side chains. Furthermore, it raises questions on the biological reasons for predominance of these post-translationally modified residues, two (Gla^3 and Gla^4) of which have been shown to be important to the activity of these peptides (7). Since it has been demonstrated here that con-T and con-G are able to adopt the same three-dimensional structure, it is possible that the former peptide is able to adopt its biologically active conformation in the absence of divalent cations, but it requires their presence for activity.

Acknowledgments—Trudy Bond is gratefully acknowledged for the amino acid analysis. Marion Loughnan and Trudy Bond are gratefully acknowledged for the venom extraction.

REFERENCES

1. McIntosh, J. M., Olivera, B. M., Cruz, L. J., and Gray, W. R. (1984) *J. Biol. Chem.* **259,** 14343–14346
2. Haack, J. A., Rivier, J., Parks, T. N., Mena, E. E., Cruz, L. J., and Olivera, B. M. (1990) *J. Biol. Chem.* **265,** 6025–6029
3. Myers, R. A., Cruz, L. J., Rivier, J. E., and Olivera, B. M. (1993) *Chem. Rev.* **93,** 1923–1936
4. Chandler, P., Pennington, M., Maccecchini, M.-L., Nashed, N. T., and Skolnick, P. (1993) *J. Biol. Chem.* **268,** 17173–17178
5. Mena, E. E., Gullak, M. F., Pagnozzi, M. J., Richter, K. E., Rivier, J., Cruz, L. J., and Olivera, B. M. (1990) *Neurosci. Lett.* **118,** 241–244
6. Skolnick, P., Boje, K., Miller, R., Pennington, M., and Maccecchini, M.-L. (1992) *J. Neurochem.* **59,** 1516–1521
7. Zhou, L.-M., Szendrei, G. I., Fossom, L. H., Maccecchini, M.-L., Skolnick, P., and Otvos, L. J. (1996) *J. Neurochem.* **66,** 620–628
8. Nishiuchi, Y., Nakao, M., Nakata, M., Kimura, T., and Sakakibara, S. (1993) *Int. J. Peptide Protein Res.* **42,** 533–538
9. Rivier, J., Galyean, R., Simon, L., Cruz, L. J., Olivera, B. M., and Gray, W. R. (1987) *Biochemistry* **26,** 8508–8512
10. Cruz, L. J., Gray, W. R., Yoshikami, D., and Olivera, B. M. (1985) *J. Toxicol. Toxin Rev.* **4,** 107–132
11. Stenflo, J., Fernlund, P., Egan, W., and Roepstorff, P. (1974) *Proc. Natl. Acad. Sci. U. S. A.* **71,** 2730–2733
12. Colpitts, T. L., Prorok, M., and Castellino, F. J. (1995) *Biochemistry* **34,** 2424–2430
13. Soriano-Garcia, M., Padmanabhan, K., deVos, A. M., and Tulinsky, A. (1992) *Biochemistry* **31,** 2554–2566
14. Cruz, L. J., Ramilo, C. A., Corpuz, G. P., and Olivera, B. M. (1992) *Biol. Bull.* **183,** 159–164
15. Schnölzer, M., Alewood, P., Jones, A., Alewood, D., and Kent, S. B. H. (1992) *Int. J. Peptide Protein Res.* **40,** 180–193
16. Jones, A., Bingham, J.-P., Gehrmann, J., Bond, T., Loughnan, M., Atkins, A., Lewis, R. J. and Alewood, P. F. (1996) *Rapid Commun. Mass Spectrosc.* **10,** 138–143
17. Chakrabartty, A., Kortemme, T., Padmanabhan, S., and Baldwin, R. L. (1993) *Biochemistry* **32,** 5560–5565
18. Rance, M., Sørensen, O. W., Bodenhausen, G., Wagner, G., Ernst, R. R., and Wüthrich, K. (1983) *Biochem. Biophys. Res. Commun.* **177,** 479–485
19. Jeener, J., Meier, B. H., Bachmann, P., and Ernst, R. R. (1979) *J. Chem. Phys.* **71,** 4546–4553
20. Kumar, A., Ernst, R. R., and Wüthrich, K. (1980) *Biochem. Biophys. Res. Commun.* **95,** 1–6
21. Bax, A., and Davis, D. G. (1985) *J. Magn. Reson.* **65,** 355–360
22. Piotto, M., Saudek, V., and Sklenár, V. (1992) *J. Biomol. NMR* **2,** 661–665
23. Wüthrich, K. (1986) *NMR of Proteins and Nucleic Acids*, Wiley-Interscience, New York
24. Pardi, A., Billeter, M., and Wüthrich, K. (1984) *J. Mol. Biol.* **180,** 741–751
25. Brünger, A. T., Clore, G. M., Gronenborn, A. M., and Karplus, M. (1986) *Proc. Natl. Acad. Sci. U. S. A.* **83,** 3801–3805
26. Brünger, A. T. (1992) *X-PLOR Manual version 3.1.,* Yale University, New Haven, CT
27. Brooks, B., Bruccoleri, R., Olafson, B. O., States, D., Swaminathan, S., and Karplus, M. (1983) *J. Comp. Chem.* **4,** 187–217
28. Pallaghy, P. K., Duggan, B. M., Pennington, M. W., and Norton, R. S. (1993) *J. Mol. Biol.* **234,** 405–420
29. Hyberts, S. G., Goldberg, M. S., Havel, T. S., and Wagner, G. (1992) *Protein Sci.* **1,** 736–751
30. Reynolds, I. J. (1990) *J. Pharmacol. Exp. Ther.* **255,** 1001–1007
31. Saacan, A. I., and Johnson, K. M. (1990) *Mol. Pharmacol.* **38,** 705–710
32. Pastore, A., and Saudek, V. (1990) *J. Magn. Reson.* **90,** 165–176
33. McLeish, M. J., Nielsen, K. J., Najbar, L. V., Wade, J. D., Lin, F., Doughty, M. B., and Craik, D. J. (1994) *Biochemistry* **33,** 11174–11183
34. Nielsen, K. J., Hill, J. M., Anderson, M. A., and Craik, D. J. (1996) *Biochemistry* **35,** 369–378
35. Seidemann, R., and Dulog, L. (1986) *Makromol. Chem.* **187,** 2545–2551
36. Smyth, M. L., Nakaie, C. R., and Marshall, G. R. (1995) *J. Am. Chem. Soc.* **117,** 10555–10562
37. Merutka, G., Dyson, H. D., and Wright, P. E. (1995) *J. Biomol. NMR* **5,** 14–24

Determination of the Solution Structures of Conantokin-G and Conantokin-T by CD and NMR Spectroscopy

Niels Skjærbæk, Katherine J. Nielsen, Richard J. Lewis, Paul Alewood and David J. Craik

J. Biol. Chem. 1997, 272:2291-2299.